ELSEVIER

Materials Science and Engineering A 454–455 (2007) 662–666

MATERIALS SCIENCE & ENGINEERING A

www.elsevier.com/locate/msea

The role of dense dislocation walls on the deformation response of aluminum alloyed hadfield steel polycrystals

D. Canadinc [a], H. Sehitoglu [a,*], H.J. Maier [b]

[a] *University of Illinois at Urbana-Champaign, Department of Mechanical and Industrial Engineering, 1206 W. Green Street, Urbana, IL 61801, USA*
[b] *University of Paderborn, Lehrstuhl f. Werkstoffkunde, D-33095 Paderborn, Germany*

Received 28 September 2005; received in revised form 15 November 2006; accepted 16 November 2006

Abstract

The deformation response and texture evolution of aluminum alloyed Hadfield steel polycrystals is explored in the presence of high-density dislocation walls. A recently developed visco-plastic self-consistent model accounting for the contribution of the dense dislocation walls to strain hardening was utilized in predicting the room temperature deformation response under tension and the accompanying texture evolution. The model successfully predicted the experimental results, demonstrating the utility of the model for polycrystals. Monitoring the texture evolution provided an independent check and validation of the model.

Keywords: Hadfield steel; Strain hardening; Crystal plasticity; Texture evolution; Microstructure; Dislocation walls; Polycrystal

1. Introduction

In a recent study, we have established a model that successfully predicts the tensile deformation response of aluminum alloyed Hadfield steel (HSwAl) single crystals [1]. The appeal of the model lies in the simplicity of the constitutive formulation utilized to predict the deformation response of the HSwAl single crystals in the presence of high-density dislocation walls (HDDWs). The key finding in single crystals is that the density of HDDWS evolves with deformation leading to a very high strain hardening rate in these materials. Depending on the crystallographic orientation the number of HDDWs varies with the effect highest in multiple slip orientations.

Prior to our work on Hadfield steel single crystals, the HDDWs had been observed in pure face-centered cubic (fcc) metals and body-centered cubic (bcc) alloys [2–10]. These works demonstrated the interaction of active slip systems with HDDWs resulting in an increased hardening. Our recent study [1] confirmed these previous observations and provided a simple model to capture the stress–strain response and evolution of HDDW volume fraction. An extension of the results to polycrystals has not been undertaken previously and will be considered in this work.

In the present work, the purpose is to extend the model [1], originally developed for single crystals of HSwAl, to the polycrystalline case utilizing the single crystal parameters and constants. To accomplish this, the deformation response of the polycrystalline samples of HSwAl and the texture evolution was measured experimentally. The deformation response and the texture change were predicted utilizing the recently developed model. The model uses a crystal plasticity framework with dislocation evolution and increased hardening associated with the presence of HDDWs. The model captured the room temperature tensile deformation response of the HSwAl polycrystals as well as the accompanying texture evolution. The results provide ground for extending the use of the model to other metallic alloys displaying HDDWs.

2. Experimental observations and mechanisms

In our previous work [1], we investigated the formation and evolution of HDDWs through a detailed transmission electron microscopy (TEM) study. Single crystals of several orientations were examined under TEM at various stages of deformation in order to shed light onto the role of HDDWs on the rapid strain hardening exhibited by HSwAl. The HDDWs are present at all stages of deformation, from small (Fig. 1(a)) to higher strain levels (Fig. 1(b)). The HDDWs reside predominantly on the {1 1 1} planes in the fcc materials. As the deformation progresses, the

* Corresponding author. Tel.: +1 217 333 4112; fax: +1 217 244 6534.
E-mail address: huseyin@uiuc.edu (H. Sehitoglu).

0921-5093/$ – see front matter © 2006 Elsevier B.V. All rights reserved.
doi:10.1016/j.msea.2006.11.122

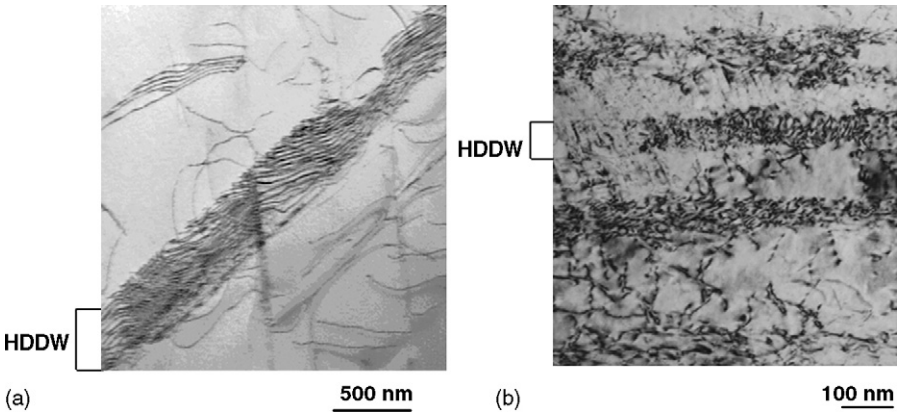

Fig. 1. TEM images showing the HDDWs and localized dislocation activities in single crystals under monotonic tensile loading. (a) HSwAl ⟨1 1 1⟩ orientation at 3% strain: early stages of HDDW formation. (b) HSwAl ⟨1 2 3⟩ orientation at 40% strain: the local density of dislocations trapped in the HDDWs becomes higher at larger strains.

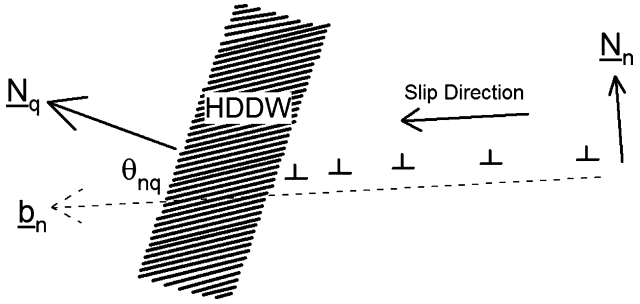

Fig. 2. A schematic showing the interaction between a HDDW that formed parallel to the plane of the active slip system (q) and another active slip system (n) within a single crystal (or grain).

volume fraction of HDDWs increases through the mutual trapping of glide dislocations due to the interaction of HDDWs with the active slip systems (Fig. 2). The dislocation density of the HDDWs is very high at the final stages of deformation, right before fracture.

The interaction of HDDWs with the active slip systems is illustrated in the schematic shown in Fig. 2 [1]. The interaction takes place simply because the HDDWs block the glide of dislocations on an active slip system. As plastic deformation progresses, a set of HDDWs that reside on the active slip system q (with the plane normal $\underline{N}_q$) forms, and the HDDWs evolve with increasing strain. An HDDW may intersect the path of dislocations moving on the plane of another active slip system n (with the plane normal $\underline{N}_n$) in the direction as specified by the burgers vector $\underline{b}_n$. This results in the trapping of the dislocations on the slip system n in the HDDWs. The angle θ_{nq} between the vectors $\underline{b}_n$ and $\underline{N}_q$ constitutes a measure of this blockage of glide dislocations by HDDWs. When the HDDWs and the slip system n are coplanar the interference is minimized as manifested through the angle θ_{nq}.

3. Modeling

The present model utilizes a crystal plasticity description of the strain rate at the single crystal level, and the reference stress evolves with the dislocation density. In the current model, the HDDW-slip system interaction is incorporated into the overall rate of dislocation density ($\dot{\rho}$) in the following format:

$$\dot{\rho} = \sum_n \{k_1\sqrt{\rho} - k_2\rho\}\left|\dot{\gamma}^n\right| + \sum_n\sum_q \frac{K}{db}\cos\theta_{nq}\left|\dot{\gamma}^n\right| \tag{1}$$

where k_1 and k_2 are constants, K is a geometric constant [1,11,12], α is the dislocation interaction parameter [13,14], and b represents the burgers vector. The first term $\sum_n\{k_1\sqrt{\rho} - k_2\rho\}|\dot{\gamma}^n|$ represents the a thermal (statistical) storage of moving dislocations ($k_1\sqrt{\rho}$) and dynamic recovery ($-k_2\rho$) in the domains outside the HDDWs [12], whereas the second term $\sum_n\sum_q \frac{K}{db}\cos\theta_{nq}|\dot{\gamma}^n|$ accounts for the contribution due to HDDWs formed parallel to the plane of the slip system q acting as effective obstacles to the moving of dislocations gliding on the active slip system n (Fig. 2). In other words, the second term represents an empirical geometric storage of dislocations due to HDDWs, which subdivide the grains and thereby decrease the mean free path of dislocations [12]. The angle θ_{nq} is the angle between the direction of slip in the active slip system n and the normal to the plane of the slip system q, and is incorporated as a measure of the interaction between HDDWs and glide dislocations in a geometric sense. The angle θ_{nq} is a variable, such that it can take different values depending on the active slip systems and the HDDWs they interact with. Moreover, the θ_{nq} continues to change as the deformation progresses due to the rotation of HDDWs in the matrix. The term d represents the average spacing between the dislocation sheets. The term $\dot{\gamma}^n$ stands for the rate of shear in the active slip system n.

By only accounting for the change in the overall rate of dislocation density (Eq. (1)), the model falls short of accounting for the rapid strain hardening of the HSwAl. The HDDWs are treated as impenetrable barriers to dislocation motion, acting as hard phases in the matrix, similar to precipitates. Accordingly, HDDWs are modeled as (elongated) ellipsoidal inclusions in the matrix. As plastic strain progresses, Orowan loops are stored around the HDDWs, giving rise to long-range internal stresses in the matrix [12]. This additional hardening (τ^B) due to HDDWs

acting as hard phases in the matrix is included through the term:

$$\tau^B = 2f\xi\mu\sum_n |\gamma^n| \tag{2}$$

where the terms μ, ξ, and f stand for the shear modulus, the Eshelby accommodation factor (elongated ellipsoidal inclusions) [15], and the volume fraction of HDDWs, respectively. The $\sum_n \gamma^{(n)}$ term is simply the summation of the shear strains on the active slip systems and represents the total matrix mismatch strain brought about by the high density dislocation sheets. The volume fraction of HDDWs (f) is a variable, and accounts for the evolution of HDDWs with increasing plastic deformation. As the plastic deformation progresses, more glide dislocations are trapped at their boundaries, adding to the overall volume fraction of HDDWs [1].

Following the incorporation of the additional hardening terms due to the HDDWs, the original rate of flow stress $\dot{\tau}$ defined in the traditional Taylor hardening format as

$$\dot{\tau} = \frac{\alpha\mu b\dot{\rho}}{2\sqrt{\rho}} \tag{3}$$

becomes

$$\dot{\tau} = \sum_n \left[\frac{\alpha^2\mu^2 bK}{4t(\tau-\tau_0)} \frac{f}{1-f} \sum_q \cos\theta_{nq} + 2f\xi\mu + \left\{ \theta_0 \left(\frac{\tau_s - \tau}{\tau_s - \tau_0} \right) \right\} \right] |\dot{\gamma}^n| \tag{4}$$

where $\{\theta_0(\tau_s - \tau/\tau_s - \tau_0)\}$ is the well-known Voce hardening term, with τ_0 as the reference strength, and τ_1, θ_0 and θ_1 as the parameters that define the hardening.

With respect to the solution of the stresses and strains at the macroscopic level, defining the deviations in strain rate and stress between the local (single crystal level) values and the overall (polycrystalline) magnitudes as

$$\tilde{\dot{\varepsilon}}_k = \dot{\varepsilon}_k - \dot{E}_k \tag{5}$$

$$\tilde{\sigma}_j = \sigma_j - \Sigma_j \tag{6}$$

where $\dot{E}$ and Σ are the polycrystal strain rate and applied stress, and $\dot{\varepsilon}_k$ and σ_j stand for the local (single crystal or grain level) strain rate and stress. Utilizing the Eshelby's inhomogeneous inclusion formulation one can solve the stress equilibrium to derive the following interaction equation:

$$\tilde{\dot{\varepsilon}} = -\tilde{M} : \tilde{\sigma} \tag{7}$$

The interaction tensor $\tilde{M}$ is defined as

$$\tilde{M} = n'(I - S)^{-1} : S : M^{(\mathrm{sec})} \tag{8}$$

where $M^{(\mathrm{sec})}$ is the secant compliance tensor for the polycrystal aggregate and S is the viscoplastic Eshelby tensor.

4. Experimental techniques

The material investigated in this study is an aluminum alloyed Hadfield steel with a chemical composition of 13.93 wt.% Mn, 1.17 wt.% C, 2.58 wt.% Al and balance Fe, and a fcc structure. Sufficient amount of impurities to influence the deformation response was not detected in the microstructure. Homogenization of the material was carried out at 1323 K for 20 h in a vacuum sealed furnace, followed by a heat treatment of 500 °C for 30 min (water quenched) to ensure optimum strength and ductility. Electro-discharge machining (EDM) was utilized to cut small-scale dog-bone shaped tension specimens. The samples were tested utilizing an Instron test frame equipped with an Instron controller. A miniature MTS extensometer was employed for accurate strain measurement in the gauge section. The experiments were conducted at slow strain rates 4×10^{-4} 1/s. Samples were analyzed with X-ray diffraction (XRD) to experimentally determine the textures in the loading direction before and after deformation.

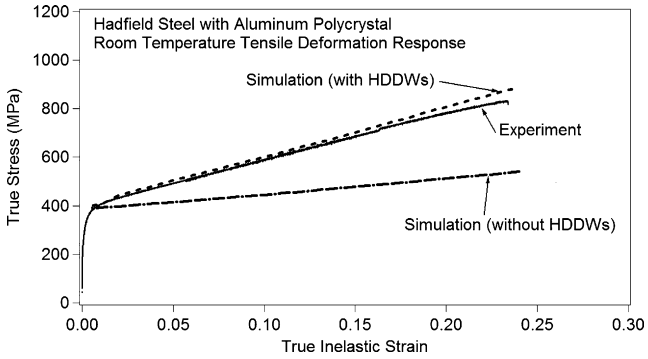

Fig. 3. The room temperature deformation response of HSwAl polycrystals.

5. Deformation response and simulations

The room temperature stress–strain response of Hadfield steel with aluminum (HSwAl) is shown in Fig. 3. Although the material has a lower carbon content (1.17 wt.%) than the single crystals of Hadfield steel previously studied (1.30 wt.%) [1], a high coefficient of deformation hardening (G/29[1]) was displayed by the polycrystals, indicating a rapid strain hardening due to the existence of HDDWs.

The stress–strain response of the HSwAl polycrystals was predicted by applying the recently developed [1] model. The experimentally measured initial texture was used as an input to the model and was allowed to evolve with deformation. The tensile deformation response was successfully captured by the model as noted in Fig. 3. The constants and hardening parameters used in predicting the deformation response of HSwAl polycrystals are given in Table 1.

In order to demonstrate the role of HDDWs on the macroscopic deformation behavior, the same model was used to predict the room temperature tensile stress–strain response in the absence of HDDWs. Therefore, the modifications allowing the current model to take HDDWs into consideration were removed. The results confirm the necessity of the incorporation of HDDWs into the model to predict the experimental deformation

[1] The coefficient of deformation hardening is normalized by the shear modulus G.

Table 1
Numerical values of constants used in the model

Constant	Numerical value
b (m)	2.58×10^{-10}
d (m)[a]	6×10^{-7}
ξ	0.4
α	0.4
K	8×10^{4}
τ_0 (MPa)	132

The units are given in square brackets. ξ, α, and K are dimensionless quantities [1].
[a] An average value was assigned to this parameter based on the microstructural observations [1].

response of the material and the associated rapid strain hardening (Fig. 3).

Utilizing the current model the texture evolution was also monitored, to independently check the capability of the model. An additional purpose was to study the role of the HDDWs on the texture evolution. For an fcc crystal oriented with the tensile axis in the primary triangle the tensile axis rotates toward the [1 1 0] direction, until it reaches the (0 0 1)–(1 1 1) boundary, along which the primary and conjugate systems are equally favored. Afterwards, simultaneous [1 0 1] and [1 1 0] slip causes rotation toward the [1 1 2] orientation (Fig. 4) [16]. However, in the case of overshooting, the rotation continues toward the [1 1 0] orientation after the tensile axis reaches the (0 0 1)–(1 0 1) boundary. As for the fcc polycrystalline aggregates with only slip as the active deformation mechanism, the general tendency under tensile loading is that the rotation takes place toward the (0 0 1)–(1 1 1) boundary, with higher intensities near the (0 0 1) and (1 1 1) poles.

With regards to representing the textures, the preference of a crystallographic orientation over the other(s) or a tendency towards a pole in a given texture is most easily represented by "texture intensity". The texture intensity is obtained by the normalization of densities of the orientations (or poles). There exist two ways of normalization: to a value of 1.0 for the average; or to a value of 1.0 for the integral [17]. The former method was utilized throughout this study.

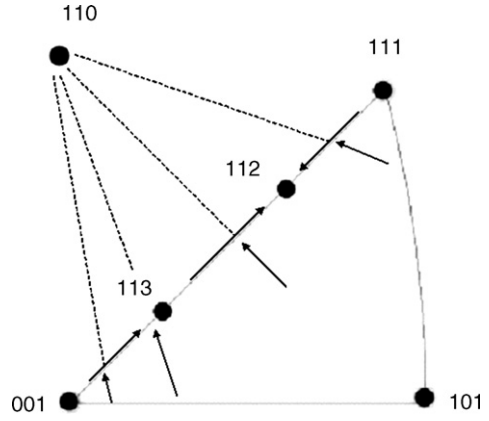

Fig. 4. Theoretically expected texture evolution in fcc crystals (after Hosford [16]). Rotation towards the 1 1 0 pole is followed by further rotation towards the 1 1 2 pole at the 0 0 1–1 1 1 boundary.

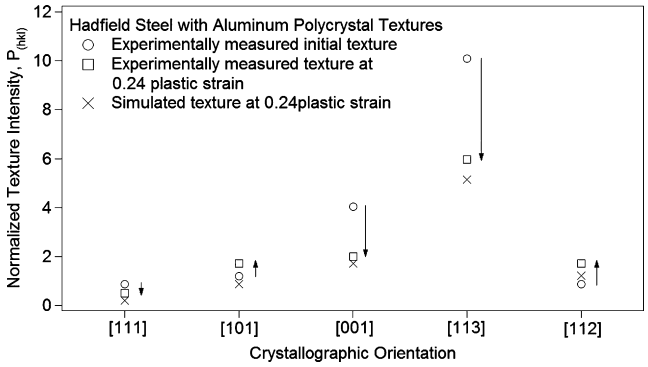

Fig. 5. Figure showing the comparison between selected orientations of experimental and numerical textures after deformation, and the initial texture in terms of their textural strengths. The selected orientations can be seen in Fig. 4. The arrows indicate the direction of change between the initial and final states of texture intensities for the specified orientations.

In three dimensional space, an orientation can be described by three angles Ψ, Θ and Φ, which are the Euler angles [16]. Let (α, β, λ) represents a specific point with α, β and λ corresponding to specific values of Ψ, Θ and Φ in an orientation space represented by the three Euler angles. The total intensity of diffracted X-rays measured at the point (α, β, λ) on an ($h\,k\,l$) pole figure comes from all crystals in the sample satisfying the Bragg condition [17]. For the ($h\,k\,l$) pole, the total pole density from crystals satisfying the Bragg condition is given (in the normalized form) by

$$P_{(h\,k\,l)}(\alpha, \beta) = \frac{1}{2\pi} \int_0^{2\pi} F(\Psi, \Theta, \Phi) \mathrm{d}\Gamma \tag{9}$$

where Γ denotes the path through the orientation distribution (OD) corresponding to rotation about the ($h\,k\,l$) pole, and F is the OD [17].

Fig. 5 shows normalized texture intensities of selected orientations for the experimentally measured initial and post-deformation textures, and the numerically calculated deformation texture. Considering the strain levels attained (0.23), we represent the texture evolution in this unconventional way for the sake of clarity. Texture evolution is usually represented more clearly with the conventional ways in the case of strains at around 2.0 or higher.

Both the simulations and the experimentally determined textures corresponding to the deformed state of the material confirm a rotation towards the [1 1 2] orientation. Similarly, the intensity of the [1 1 3] orientation prominent in the initial texture decreases significantly due to tensile deformation. The agreement between the numerical and experimental results point at the capability of the modeling effort presented herein. Nevertheless, at this time, the focus of this paper is placed on modeling the macroscopic deformation response of the HSwAl polycrystals.

6. Final remarks and discussion of results

A microstructure based model originally developed for single crystals [1], has been utilized to predict the deformation response and texture evolution of the HSwAl polycrystals. The information regarding the orientation of HDDWs in the 3D

space was obtained though conventional trace analysis and TEM [1], and incorporated into the current model. In the current material, different sets of HDDWs are allowed to form in numerous grains. The simulations were conducted by representing the HDDWs of the polycrystalline aggregate similar to that of the single crystals oriented in the ⟨1 1 1⟩ direction [1]. The HDDWs form if a large fraction of the shear in a grain (or crystal) occurs when two slip systems on the same slip plane are active [2], and the direction of the HDDWs is dictated by the slip planes, which experience large coplanar slip [1,2]. Such observations are made on ⟨1 1 1⟩ oriented single crystals, where multiple slip is the deformation mechanism resulting in two sets of HDDWs.

We chose the modeling parameters and constants for the ⟨1 1 1⟩ orientated single crystals of the HSwAl to predict the deformation response of polycrystals of the same material. Allowing a tensile (or compressive) stress in the ⟨1 1 1⟩ direction of an fcc metal produces a corner in the 'plastic potential' as defined by Kocks and colleagues where the facets of six slip systems meet in the five-dimensional deviatoric stress space [1,17]. Six slip systems can be simultaneously activated, making the ⟨1 1 1⟩ orientation a multi-slip orientation in fcc metals and suitable as a basis for predicting polycrystalline response. Such highly symmetric situations are not possible with any other orientation for an fcc material. The close prediction of the deformation response and texture evolution with the modified VPSC model validates our approach.

Another noteworthy point is the small difference between the chemical composition of the material used in this study and our previous work [1]. The single crystals of HSwAl had 1.30 wt.% C in the composition, whereas the current material has 1.17 wt.% C other elements being the same (except for Fe, which constitutes the balance). Mechanical experiments revealed lower strength levels for the 1.17 wt.% C case compared to the 1.30 wt.% C. The reference strength value was changed from 159 [1] to 132 MPa in the simulations, while the remainder of the constants and hardening parameters in the constitutive relationship remained the same as in the original single crystal model [1].

7. Conclusions

In the present study, the room temperature tensile deformation response of polycrystals of aluminum alloyed Hadfield steel is studied. We draw the following conclusions:

1. The recently introduced model originally established for single crystals of aluminum alloyed Hadfield steel in the presence of high density dislocation walls (HDDW) was applied to polycrystals of the same material. The results point at the success of the model and confirm its applicability to the polycrystals, providing a venue for its use with other materials that display HDDWs.
2. Specifically, the microstructure based model successfully captured the texture evolution imposed by the tensile deformation, as well as the magnitude of the strain hardening coefficient which is of the order of G/20 in these class of alloys.

Acknowledgement

This work was supported by the National Science Foundation grant DMR-0313489.

References

[1] D. Canadinc, H. Sehitoglu, H.J. Maier, Y.I. Chumlyakov, Acta Mater. 53 (2005) 1831.
[2] G. Winther, D. Juul Jensen, N. Hansen, Acta Mater. 45 (1997) 5059.
[3] N. Hansen, D. Juul Jensen, Acta Metall. Mater. 40 (1992) 3265.
[4] D. Juul Jensen, N. Hansen, Acta Metall. Mater. 38 (1990) 1369.
[5] B. Peeters, S.R. Kalidindi, P. Van Houtte, E. Aernoudt, Acta Mater. 48 (2000) 2123.
[6] B. Peeters, M. Seefeldt, P. Van Houtte, E. Aernoudt, Scripta. Mater. 45 (2001) 1349.
[7] G. Winther, In: Proceedings of the 19th Risø international symposium on materials science, Denmark, 1998, p. 185.
[8] J.L. Raphanel, J.H. Schmitt, B. Baudelet, In: Proceedings of the 8th Risø international symposium on materials science, Denmark, 1992, p. 491.
[9] Q. Liu, D. Juul Jensen, N. Hansen, Acta Mater. 46 (1998) 5819.
[10] Q. Liu, N. Hansen, Phys. Status Solidi. A 149 (1995) 187.
[11] D. Canadinc, MS Thesis, University of Illinois at Urbana-Champaign, USA, 2001.
[12] D. Canadinc, I. Karaman, H. Sehitoglu, Y.I. Chumlyakov, H.J. Maier, Metall. Mater. Trans. A 43 (2003) 1821.
[13] J.A. Venables, J. Phys. Chem. Solids 25 (1963) 693.
[14] G. Saada, Acta Metall. 8 (1960) 841.
[15] L.M. Brown, D.R. Clarke, Acta Metall. 23 (1975) 821.
[16] W.F. Hosford, The Mechanics of Crystals and Textured Polycrystals, Oxford University Press, New York, 1993.
[17] U.F. Kocks, C.N. Tome, H.R. Wenk, Texture and Anisotropy, 2nd ed., Cambridge University Press, 2000.